

Artificial neural network modeling for predicting elastic strain of white birch disks during drying

Zongying Fu^{1,2} · Stavros Avramidis² · Jingyao Zhao¹ · Yingchun Cai¹

Received: 11 January 2016 / Published online: 12 April 2017
© Springer-Verlag Berlin Heidelberg 2017

Abstract Elastic strain is one of the most important parameters associated with drying stresses. The research presented in this paper attempts to develop an artificial neural network based model for predicting elastic strain in white birch (*Betula platyphylla* Suk) disks during drying as a function of temperature, moisture content, relative humidity and distance from the pith. The data set was obtained by using image analysis method under two drying schedules and divided into three subsets for training (60%), validation (20%) and test (20%). According to the results, the values of determination coefficient (R^2) obtained were greater than 0.97, 0.96 and 0.95 for the training, validation and test sets, respectively.

1 Introduction

Defects in lumber often occur during kiln drying and they tend to reduce value, application potential and utilization (Simpson 2001). Their cause is often linked to drying stresses that are produced by moisture content decrease and wood shrinkage anisotropy (Fu et al. 2015). As an important variable that affects product quality, extensive studies on drying stresses have been carried out. Svensson (1995, 1996) and Svensson and Mårtensson (1999, 2002) investigated the strain and shrinkage forces perpendicular to grain

in wood under controlled drying conditions and different mechanical restraint schemes and also using a model for simulation. In a similar research by Lazarescu et al. (2009, 2010) and Lazarescu and Avramidis (2010), an empirical model was built and used to quantify the drying stresses based on the developed strain set. Perré and Passard (2004) proposed a comprehensive model to predict drying stresses evolution based on mechano-sorptive creep at different temperature levels. Moutee et al. (2005, 2007) developed a rheological model of wood cantilever for emulating drying stresses and creep behavior at various load levels and ambient conditions. A number of investigations about drying stresses have also been reported in recent years (Ferrari et al. 2010; Watanabe et al. 2013a; Salinas et al. 2015).

To better understand the evolution of drying stresses, studying thin disks from wood logs is advantageous because of the possibility to control the moisture gradient better than in wood boards. Kang and Lee (2002) developed a mathematical model for the prediction of drying stresses and resultant deformation within a tree disk that was treated as a cylindrically orthotropic and radially inhomogeneous material. Larsen and Ormarsson (2013) investigated moisture-induced stresses in log cross-sections by a finite element method where moisture content profiles were assumed to be symmetric around the pith.

Within the elastic region, elastic strain of wood during drying is in good agreement with the drying stress. Thus, the drying stress of a single moment can be evaluated by the instant elastic strains. However, there are no certain relationships between ambient conditions and elastic strain. Inspired by the functional behavior of the biological nervous system, artificial neural network (ANN) modeling is particularly useful for dealing with the nonlinearities and complexities of ill-defined processes using past historical data, even if all mechanisms and principles are not clarified;

✉ Yingchun Cai
caiyinchunnefu@163.com

¹ Key Laboratory of Bio-based Material Science and Technology (Ministry of Education), College of Material Science and Engineering, Northeast Forestry University, Harbin 150040, People's Republic of China

² Department of Wood Science, University of British Columbia, Vancouver, Canada

further, the network can be built directly from experimental data by the self-organizing capabilities without any prior assumptions (Aghbashlo et al. 2015). In general, the basic information processing elements of the neural network operation are called neurons. Some of the neurons interface with the outside world to receive information called input layer, and other neurons communicate the prediction to the outside world called output layer. All the rest of the neurons connect the input layer to the output layer called hidden layers. The network function is determined largely by the interconnections between neurons, which are not simple connections but some non-linear functions (Zhang and Friedrich 2003).

As a fascinating mathematical tool, ANNs have been reported in many published works and also used in the field of wood science for predicting some physical and mechanical properties, such as wood density (Iliadis et al. 2013), wood thermal conductivity (Avramidis and Iliadis 2005a), wood dielectric loss factor (Avramidis et al. 2006), hygroscopic equilibrium moisture content (Avramidis and Iliadis 2005b), compression strength of heat treated wood (Tiryaki and Aydın 2014), and bending strength and stiffness of wood (Mansfield et al. 2007). Additionally, the ANN approach has been employed in wood industry. Wu and Avramidis (2006) predicted timber kiln drying rates as a function of initial moisture content, basic density, and drying time. Ceylan (2008) simulated the variation of moisture content of poplar timber versus drying time. Watanabe et al. (2013b) evaluated the final moisture content of individual sugi samples after air-drying based on initial moisture content, basic density, annual ring orientation, annual ring width, heartwood ratio and lightness. Tiryaki et al. (2016) employed ANN for predicting surface roughness and power consumption in abrasive machining of wood. The relationships between climatic conditions and internal bond strength of particleboard were investigated using ANN by Korai and Watanabe (2016). However, no research has been published using ANN to predict drying stresses.

The objective of this study was to predict the elastic strain of wood disks during their kiln drying by means of ANN modeling where the inputs include drying temperature, moisture content, relative humidity and distance from the pith.

2 Materials and methods

Wood for this study was obtained from forests in the region of the Lesser Khingan Mountains, located in Heilongjiang Province, China. One hundred wood disks of 30 mm thickness were cut from one plantation white birch (*Betula platyphylla* Suk) tree, 22 years of age and with an average diameter of 250 mm. For one experiment, twenty wood

disks without visible defects were randomly selected from them and dried in a GDS-100 (Shanghai Scientific Instruments Yiheng Co., Ltd.) conditioning chamber at two different drying schedules. For each schedule, ten wood disks were used, of which one was used to determine the green moisture content, three for determining the three different target moisture contents (26, 18 and 10%), and the remaining six wood disks (three of them as replacement) were ready for strain studies. Two replications were carried out.

The details of the two drying schedules are shown in Fig. 1. For schedule 1, the temperature was kept at $40 \pm 1^\circ\text{C}$ and the relative humidity decreased slowly from 94 ± 2 to $57 \pm 2\%$. For schedule 2, the dry-bulb temperature started at $40 \pm 1^\circ\text{C}$, increased 2°C every 24 h above 30% moisture content and increased 2°C every 12 h below 30% moisture content, up to the final temperature of $60 \pm 1^\circ\text{C}$; the humidity decreased from 100 ± 2 to $65 \pm 2\%$.

The elastic strain was measured by an image-supported, noncontact method based on dot pitches. The camera lens (1628×1236 resolution) was fixed on a perpendicularly placed tripod and kept 200 mm from the test plane. Prior to drying, red stains (the distance between two measuring points is 20 mm in tangential direction) were sprayed on the polished surface of the disks, using oil-based pike (Fig. 2). While drying to 26, 18, and 10% moisture content, two of the wood disks were taken out and each one cut into 18 test specimens ($30 \times 10 \times 30 \text{ mm}^3$, $T \times R \times L$) along the grid lines, and also the images of the disks (including a scale-plate) were taken before and after cutting. The target moisture contents were determined by the oven-dry method.

Thereafter, the images were imported into specialized software (Image J) for measuring and analyzing the actual length of the two red stains, as shown in Fig. 2. By comparing the changes of dot pitches, the strain values can be obtained.

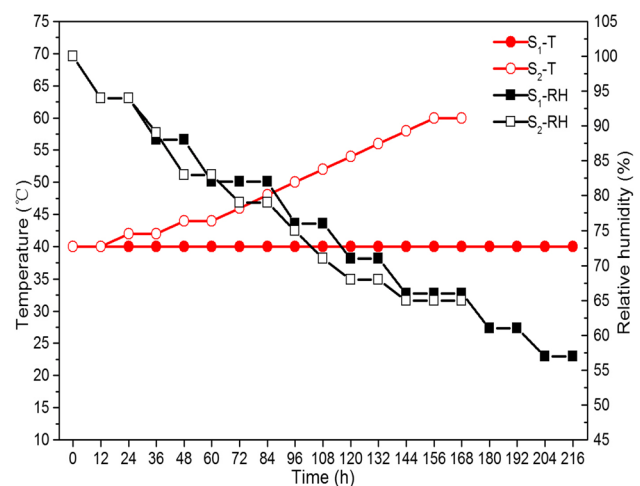
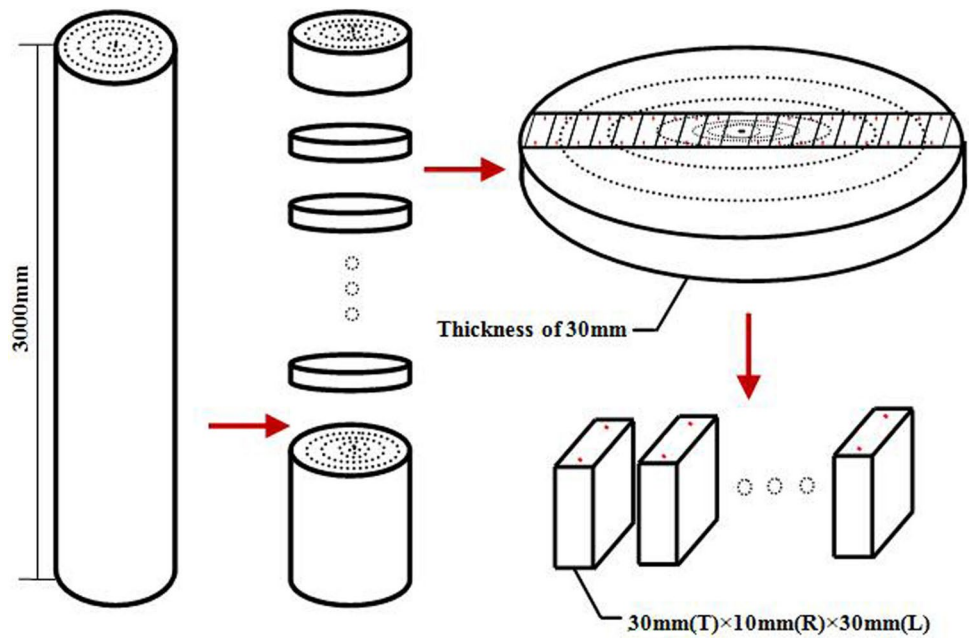


Fig. 1 Schematic of drying schedules: S_1 schedule 1; S_2 schedule 2

Fig. 2 Cutting diagram of disks and test specimens



The tangential elastic strain was calculated using the following equation:

$$\varepsilon_t = (L_1 - L_2)/L_0 \tag{1}$$

where L_0 is the distance in mm between two measuring points on the strain specimens under green conditions, L_1 is the distance in mm between two measuring points on the strain specimens before cutting at each target moisture content and L_2 is the distance in mm between two measuring points on the strain specimens after cutting test specimens ($30 \times 10 \times 30 \text{ mm}^3$, $T \times R \times L$) from wood disks.

3 Artificial neural network analysis

A three-layer feed-forward artificial neural network model trained with the back-propagation of errors algorithm was employed in this study, which has been widely used in the past (Myhara and Sablani 2001; Avramidis and Iliadis 2005a, b; Avramidis et al. 2006; Esteban et al. 2009; Tiryaki and Hamzaçebi 2014; Tiryaki and Aydın 2014). The database generated by these experiments was randomly divided into three groups without repetition, including the training group (98 test specimens, 60% of the total), the validation group (32 test specimens, 20% of the total) and the testing group (32 test specimens, 20% of the total). The division of the groups and the percentage of the data were the same as reported by other authors in the past (Myhara and Sablani 2001; Esteban et al. 2009).

The 4-6-1 neural network configuration was selected in the designed ANN model, as shown in Fig. 3. The inputs used were temperature, moisture content, relative humidity and distance from the pith, and the output was elastic strain. The optimal number of neurons in the hidden layer was adjusted during training and validation process. It is believed that the two-layer sigmoid/linear network can present any relationship between input and output if there are enough neurons in the hidden layer (Hagan et al. 1996; Zhang and Friedrich 2003). Thus, the tangent sigmoid function (Eq. 2) in the hidden layer and the linear function in the output layer were chosen as the transfer functions. Levenberg–Marquardt back propagation algorithm was chosen as the training algorithm.

$$\tan \text{sig}(x) = \frac{2}{1 + e^{-2x}} - 1 \tag{2}$$

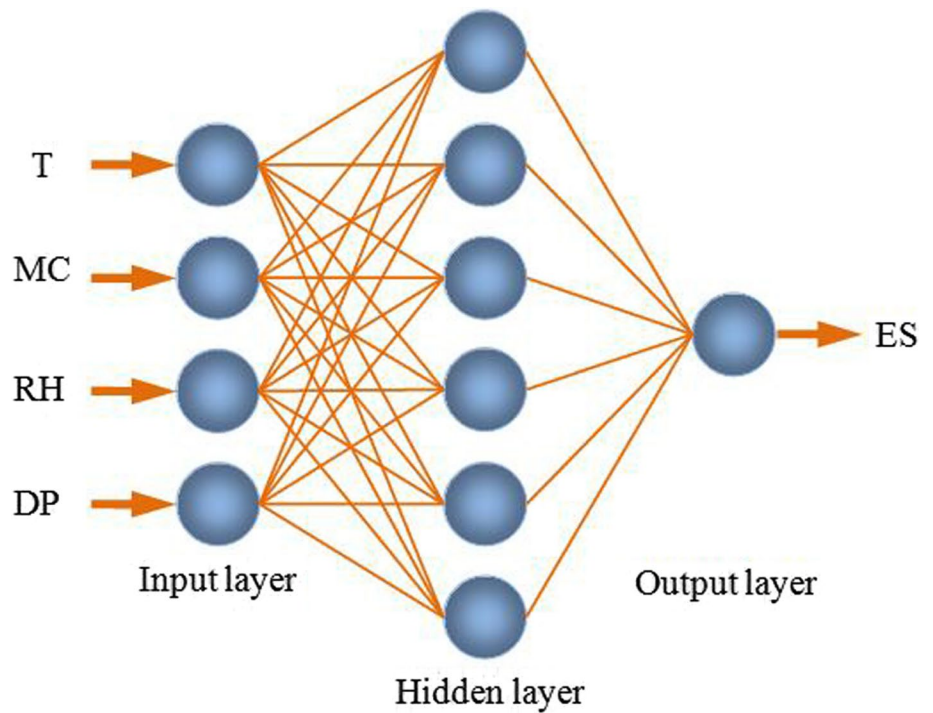
where $\tan \text{sig}(x)$ is the output value of the neuron; and x is the input value of the neuron.

The performance of the network was evaluated by the mean squared error (MSE), defined by Eq. (3). The smaller the MSE between measured and predicted values, the stronger is the predictive performance. In addition, the correlation coefficient (R) and the coefficient of determination (R^2) were also introduced to evaluate network performance.

$$MSE = \frac{1}{n} \sum_{i=1}^n (t_i - p_i)^2 \tag{3}$$

where n is the total number of data, t_i is the measured value, p_i is the predicted value.

Fig. 3 Configuration of a feedforward artificial neural network: *T* temperature, *MC* moisture content, *RH* relative humidity, *DP* distance from the pith



4 Results and discussion

In order to evaluate the performance of the neural network, *MSE* values for the training, validation and test sets versus

epochs are depicted in Fig. 4. The dashed line parallel to abscissa axis is the goal error of $1e-6$. The best validation performance is $1.21e-06$ at epoch 17. Beyond 17 iterations, the *MSE* value for validation set will increase. Furthermore,

Fig. 4 Plot of mean squared error for the training, validation and test set changes with number of iterations

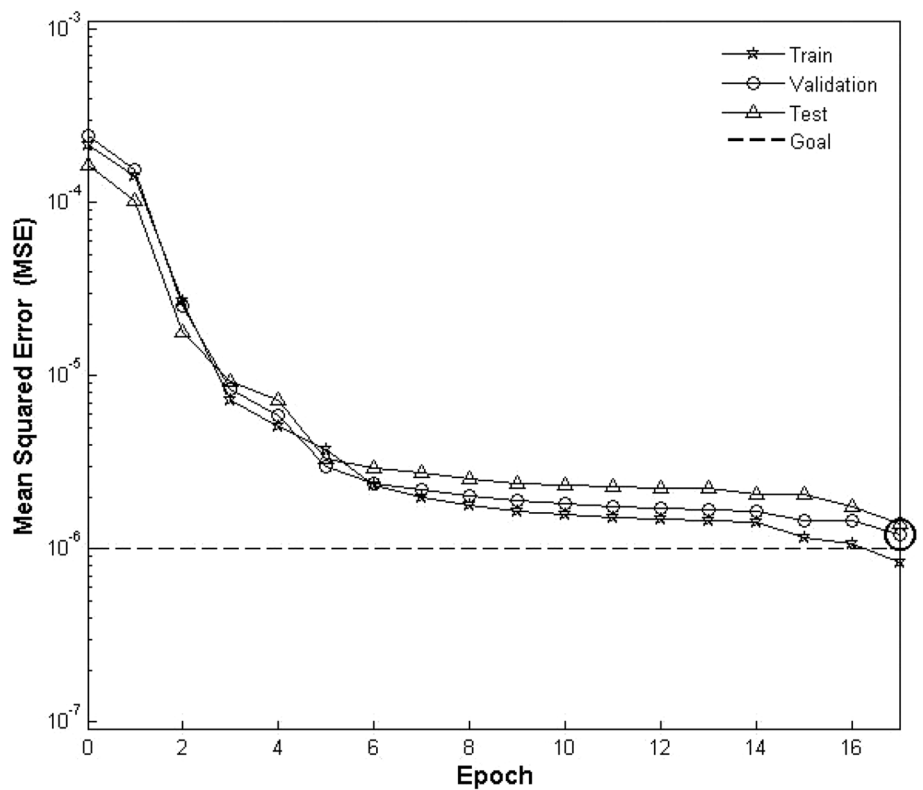


Table 1 Results of linear regression between experimental and predicted values

Set	Linear regression equation	R	R^2
Training set	Predicted = (0.98) Experimental - 7.7e-05	0.988	0.97
Validation set	Predicted = (0.95) Experimental - 0.00031	0.983	0.96
Test set	Predicted = (1) Experimental + 0.0001	0.978	0.95
All data	Predicted = (0.98) Experimental - 9.1e-05	0.985	0.97

the MSE values in the test set have similar characteristics to those in the validation set. There is no significant overfitting phenomenon, which is a serious problem in neural network training process with an increase in validation set error in conjunction with a decrease in training set error

(Sarle 1995; Hagan et al. 1996; Esteban et al. 2009). Thus, the neural network is considered to be quite reasonable.

The linear regression equation of the neural network between the experimental and predicted values for the training, validation, test and all data sets, in conjunction with their correlation coefficients (R) and determination coefficient (R^2) are presented in Table 1. These regression equations represent strong correlations between the experimental and predicted values. The values of R for the training, validation, test, all data sets are 0.988, 0.983, 0.978 and 0.985, respectively. Additionally, the value of R^2 obtained from the test set is 0.95, indicating that the network model is capable to explain more than 95% of the experimental values. In the other three sets, the values of R^2 are all greater than 0.95.

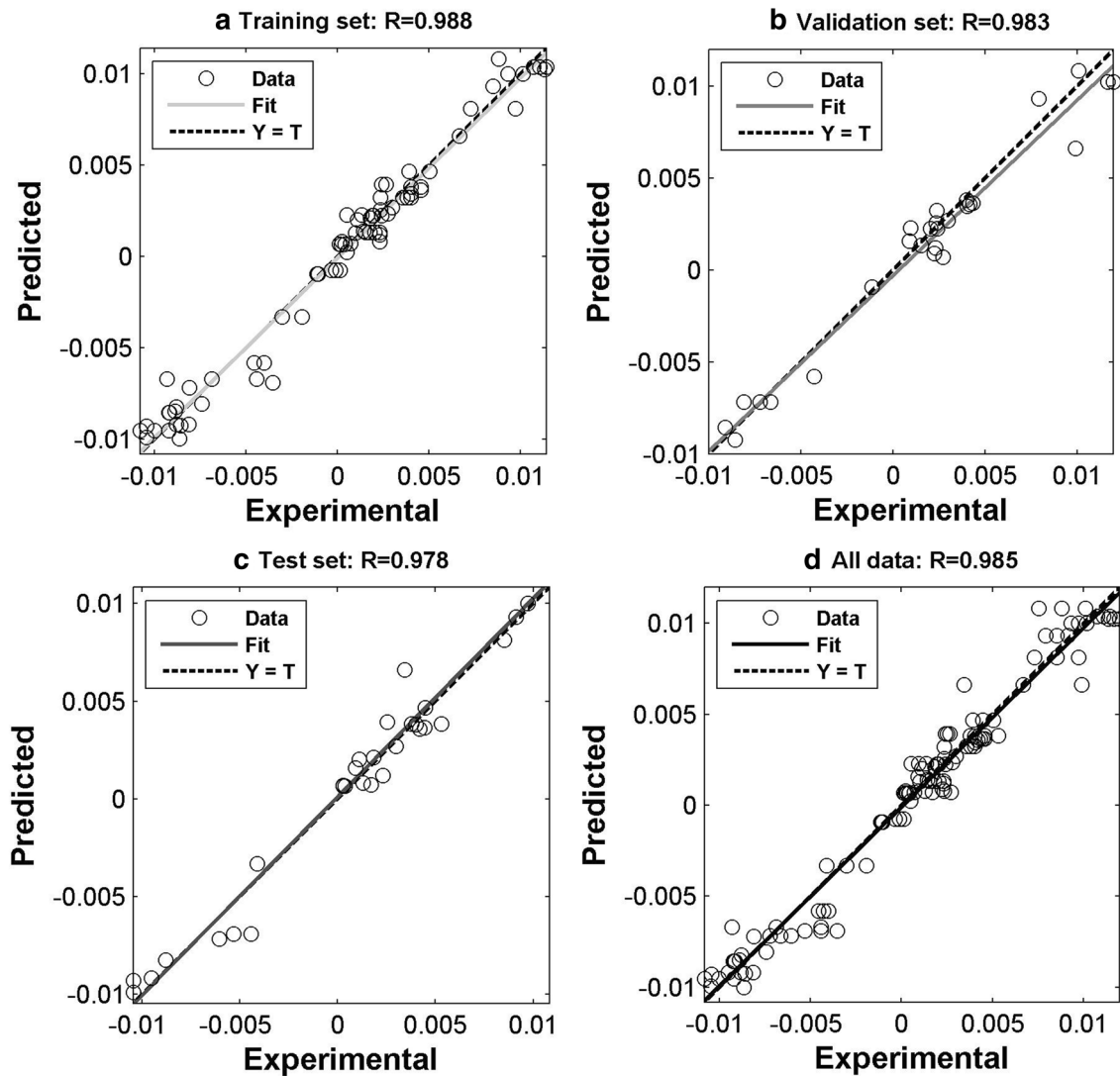


Fig. 5 Cross-correlation graph between experimental and ANN predicted values for elastic strain: **a** training set; **b** validation set; **c** test set; **d** all data. The respective regression equations and the values of R^2 are given in Table 1

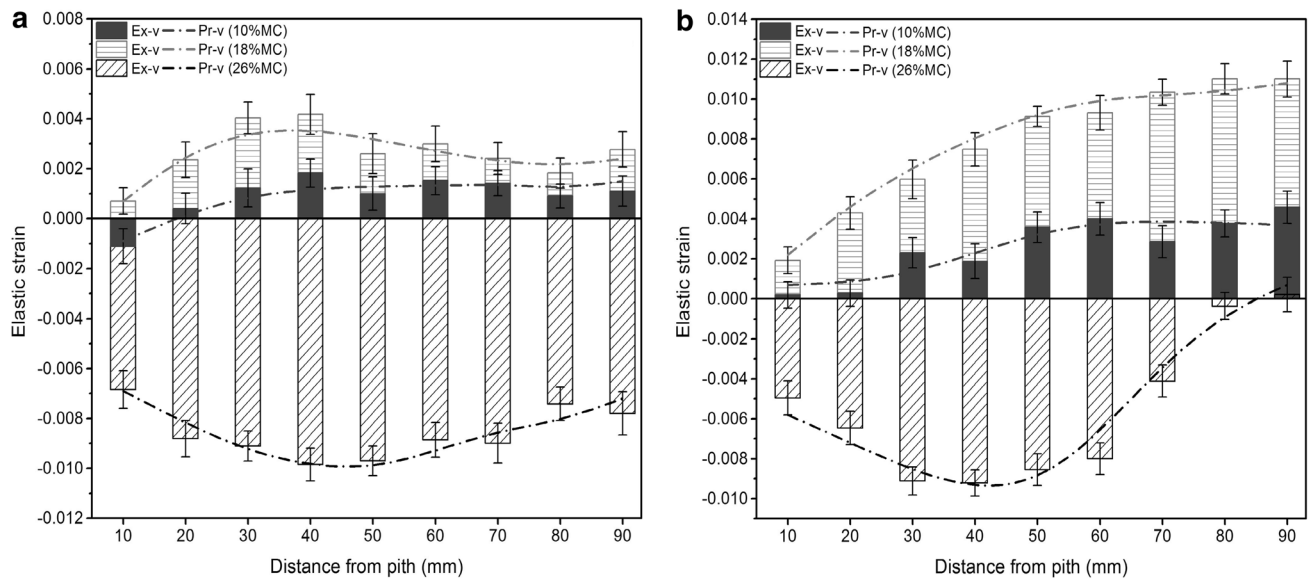


Fig. 6 Comparison of experimental and predicted values of elastic strain under two drying schedules in the test set: **a** schedule 1 **b** schedule 2

Compared with other reports where ANN was used to model other wood mechanical and physical properties, the following can be observed: Mansfield et al. (2007) reported R^2 values for MOE ranging between 0.693 and 0.750, and the corresponding MOR models ranging from 0.438 to 0.561 in western hemlock. Esteban et al. (2009) obtained an R^2 value of 0.75 in determining the modulus of elasticity of solid wood. Tiryaki and Aydın (2014) reported R^2 values that were greater than 0.99 for all of the data sets in predicting compression strength of heat treated woods.

The regression fit between the experimental and predicted values for elastic strain in the four sets is plotted in Fig. 5. As seen in this figure, the solid lines and the dashed lines exhibit a good linear fit between experimental and predicted values. In the training, test and all-data sets, the solid line is almost on top of the dashed line, denoting that the predicted values are in good agreement with the experimental values. Thus, the ANN model developed in this work can be accepted as a reliable approach to predict the elastic strain during drying.

The comparison of experimental and predicted values for elastic strain in the test set is illustrated in Fig. 6. As plotted, the experimental values of elastic strain are shown in the bar chart and the predicted values of elastic strain are depicted by the dashed line. For both of the two schedules, the tangential tensile elastic strain was shown at the moisture content of 26%, but the tensile elastic strain was replaced by the compressive elastic strain at the moisture content of 18 and 10%. Furthermore, the tensile elastic strain at 10% moisture content was smaller than the corresponding value at 18% moisture content due to the fact that the elastic modulus increased with

decreasing moisture content below the fiber saturation point (Gerhards 2007). For schedule 1, there was no clear trend for elastic strain, especially at the moisture content of 10%. Whereas, for schedule 2, the elastic strain was increased with the increasing distance from the pith at the moisture content of 18 and 10% because of the uneven distribution of moisture content and the difference of wood properties in radial direction. The comparison between the predictions and experiment results shows that almost all of the values predicted by the neural network model are very close to the experimental ones for the two drying schedules, but only a smaller deviation is observed at a distance of 70 mm from the pith at 10% moisture content in schedule 2. This result is consistent with the greater R^2 in the test set thus demonstrating the reliability of the proposed ANN model in this study.

5 Conclusion

This study presented the results of modeling elastic strain by a three-layer feedforward neural network configuration. The parameters of drying temperature, moisture content, relative humidity and distance from the pith were the independent variables. The values of R^2 in all of the sets were higher than 0.95. The value of MSE approached the goal error of $1e-6$, thus the proposed neural network model was shown to result in better performance in terms of R^2 and MSE . When the experimental measurements were compared to the predicted values, good fit was observed that supported the reliability of the proposed ANN model.

Acknowledgements This study is financially supported by the Fundamental Research Funds for the Central Universities of China (Grant No. 2572015AB08).

References

- Aghbashlo M, Hosseinpour S, Mujumdar AS (2015) Application of artificial neural networks (ANNs) in drying technology: a comprehensive review. *Dry Technol* 33(12): 1397–1462
- Avramidis S, Iliadis L (2005a) Predicting wood thermal conductivity using artificial neural networks. *Wood Fiber Sci* 37: 682–690
- Avramidis S, Iliadis L (2005b) Wood-water sorption isotherm prediction with artificial neural networks: a preliminary study. *Holz-forschung* 59:336–341
- Avramidis S, Iliadis L, Mansfield SD (2006) Wood dielectric loss factor prediction with artificial neural networks. *Wood Sci Technol* 40:563–574
- Ceylan I (2008) Determination of drying characteristics of timber by using artificial neural networks and mathematical models. *Dry Technol* 26: 1469–1476
- Esteban LG, Fernandez FG, Palacios PD (2009) MOE prediction in *Abies pinsapo* Boiss. timber: application of an artificial neural network using non-destructive testing. *Comput Struct* 87:1360–1365
- Ferrari S, Pearson H, Allegretti O, Gabbitas B (2010) Measurement of internal stress in *Radiata* pine sapwood during drying using an improved online sensor. *Holz-forschung* 64:781–789
- Fu ZY, Zhao JY, Huan SQ, Sun XM, Cai YC (2015) The variation of tangential rheological properties caused by shrinkage anisotropy and moisture content gradient in white birch disks. *Holz-forschung* 69(5):573–579
- Gerhards CC (2007) Effect of moisture content and temperature on the mechanical properties of wood: an analysis of immediate effects. *Wood Fiber Sci* 14(1):4–36
- Hagan MT, Demuth HB, Beale MH (1996) *Neural network design*. PWS Publishing Company, Boston
- Iliadis L, Mansfield SD, Avramidis S, El-Kassaby Y (2013) Predicting Douglas-fir wood density by artificial neural networks (ANN) based on progeny testing information. *Holz-forschung* 67(7):771–777
- Kang W, Lee NH (2002) Mathematical modeling to predict drying deformation and stress due to the differential shrinkage within a tree disk. *Wood Sci Technol* 36:463–476
- Korai H, Watanabe K (2016) Predicting the strength reduction of particleboard subjected to various climatic conditions in Japan using artificial neural networks. *Eur J Wood Prod*. doi:10.1007/s00107-016-1056-8
- Larsen F, Ormarsson S (2013) Numerical and experimental study of moisture-induced stress and strain field developments in timber logs. *Wood Sci Technol* 47:837–852
- Lazarescu C, Avramidis S (2010) Modeling shrinkage response to tensile stresses in wood drying: II. Stress-shrinkage correlation in restrained specimens. *Dry Technol* 28(2):186–192
- Lazarescu C, Avramidis S, Oliveira L (2009) Modeling shrinkage response to tensile stresses in wood drying: I. Shrinkage-moisture interaction in stress-free specimens. *Dry Technol* 27(11):1183–1191
- Lazarescu C, Avramidis S, Oliveira L (2010) Modeling shrinkage response to tensile stresses in wood drying: III. Stress-tensile set correlation in short pieces of lumber. *Dry Technol* 28(6):745–751
- Mansfield SD, Iliadis L, Avramidis S (2007) Neural network prediction of bending strength and stiffness in western hemlock (*Tsuga heterophylla* Raf.). *Holz-forschung* 61:707–716
- Moutee M, Fafard M, Fortin Y (2005) Modeling the creep behavior of wood cantilever loaded at free end during drying. *Wood Fiber Sci* 37(3):521–534
- Moutee M, Fortin Y, Fafard M (2007) A global rheological model of wood cantilever as applied to wood drying. *Wood Sci Technol* 41:209–234
- Myhara RM, Sablani S (2001) Unification of fruit water sorption isotherm using artificial neural networks. *Dry Technol* 19(8):1543–1554
- Perré P, Passard J (2004) A physical and mechanical model able to predict the stress field in wood over a wide range of drying conditions. *Dry Technol* 22:27–44
- Salinas C, Chavez C, Ananias RA, Elustondo D (2015) Unidimensional simulation of drying stress in *radiata* pine wood. *Dry Technol* 33(8):996–1005
- Sarle WS (1995) Stopped training and other remedies for overfitting. In: *Proceedings of the 27th Symposium on the Interface of Computing Science and Statistics*, pp 352–360
- Simpson W (2001) Chap. 08 drying defects. *USDA Agricultural Handbook No. 188: Dry Kiln Operator's Manual*. Wisconsin, Madison, pp 179–205
- Svensson S (1995) Strain and Shrinkage force in wood under kiln drying conditions. I: Equipment and preliminary results. *Holz-forschung* 49(4):363–368
- Svensson S (1996) Strain and shrinkage force in wood under kiln drying conditions. II: Measuring strains and shrinkage under controlled climate conditions. *Holz-forschung* 50(5):463–469
- Svensson S, Mårtensson A (1999) Simulation of drying stresses in wood Part I: comparison between one and two dimensional models. *Holz Roh-Werkst* 57(2):129–136
- Svensson S, Mårtensson A (2002) Simulation of drying stresses in wood Part II: convective air drying of sawn timber. *Holz Roh-Werkst* 60(1):72–80
- Tiryaki S, Aydın A (2014) An artificial neural network model for predicting compression strength of heat treated woods and comparison with a multiple linear regression model. *Constr Build Mater* 62:102–108
- Tiryaki S, Hamzaçebi C (2014) Predicting modulus of rupture (MOR) and modulus of elasticity (MOE) of heat treated woods by artificial neural networks. *Measurement* 49:266–274
- Tiryaki S, Özşahin S, Aydın A (2016) Employing artificial neural networks for minimizing surface roughness and power consumption in abrasive machining of wood. *Eur J Wood Prod*. doi:10.1007/s00107-016-1050-1
- Watanabe K, Kobayashi I, Saito S, Kuroda N, Noshiro S (2013a) Nondestructive evaluation of drying stress level on wood surface using near-infrared spectroscopy. *Wood Sci Technol* 47(2):299–315
- Watanabe K, Matsushita Y, Kobayashi I, Kuroda N (2013b) Artificial neural network modeling for predicting final moisture content of individual Sugi (*Cryptomeria japonica*) samples during air-drying. *J Wood Sci* 59:112–118
- Wu H, Avramidis S (2006) Prediction of timber kiln drying rates by neural networks. *Dry Technol* 24(12):1541–1545
- Zhang Z, Friedrich K (2003) Artificial neural networks applied to polymer composites: a review. *Compos Sci Technol* 63:2029–2044